



**HAL**  
open science

# Disentangling chaotic laminar and turbulent flow components

Damien Biau, Leonardo Rigo

► **To cite this version:**

Damien Biau, Leonardo Rigo. Disentangling chaotic laminar and turbulent flow components. 2022.  
hal-03675033v1

**HAL Id: hal-03675033**

**<https://hal.science/hal-03675033v1>**

Preprint submitted on 22 May 2022 (v1), last revised 26 May 2022 (v2)

**HAL** is a multi-disciplinary open access archive for the deposit and dissemination of scientific research documents, whether they are published or not. The documents may come from teaching and research institutions in France or abroad, or from public or private research centers.

L'archive ouverte pluridisciplinaire **HAL**, est destinée au dépôt et à la diffusion de documents scientifiques de niveau recherche, publiés ou non, émanant des établissements d'enseignement et de recherche français ou étrangers, des laboratoires publics ou privés.

# Disentangling chaotic laminar and turbulent flow components

Damien Biau\* and Leonardo Rigo

*Dynfluid Laboratory, École Nationale Supérieure d'Arts et Métiers,  
151 Boulevard de l'Hôpital, 75013 Paris, France*

Transition to turbulence generally involves successive bifurcations from steady laminar solution to spatio-temporal chaos. For the case of slightly curved duct flows, the scale separation allows to separate the Navier-Stokes equations into two sets, namely the laminar solution and turbulent fluctuations. The laminar flow is sensitive to the weak curvature and is governed by the Dean number, while the small scale turbulent disturbances are insensitive to the curvature and are governed by the Reynolds number. The laminar solution is subject to super critical bifurcation leading to temporal chaos for increasing Dean number. On the other hand, the turbulent fluctuations show a sub-critical bifurcation depending on the Reynolds number. The separation between laminar, temporally chaotic solution and turbulent disturbances allows to separate the secondary flow in accordance to Prandtl's classification. The frequency analysis of the respective head losses illustrates the nonreciprocal influence of the temporal-chaos onto the spatio-temporal turbulence.

Duct flows have been investigated for more than two centuries with the aim of tackling a wide variety of problems, from water supply to blood circulation [1]. In 1845, Stokes obtained an analytical solution for a gravity-driven flow in an inclined tube [2]. That solution was obtained assuming a steady state, namely a laminar flow. The Stokes solution gives a head loss per unit of length proportional to the bulk velocity, in agreement with observations for relatively low velocities. The departure from the Stokes solution for larger velocities was explained in 1883 by Osborne Reynolds who showed that two very different regimes of flow are present, laminar and turbulent [3]. Moreover, he showed that the transition is characterised by a single dimensionless number, called the Reynolds number by Sommerfeld [4].

In order to determine the critical Reynolds number for the flow, the linear stability analysis of the laminar solution appeared promising, especially after the successful study by Taylor on the stability analysis of a viscous liquid contained between two rotating cylinders [5]. However, for pipe flows, preliminary studies [6] provided evidence that the laminar solution is stable in a regime where turbulence is generally observed. In fact, Meseguer & Trefethen [7], with a very efficient numerical method, showed that circular pipe flows are asymptotically stable up to Reynolds number  $10^7$ , for any infinitesimal perturbations. This inconsistency between linear stability results and the observations led to question the single mode asymptotic analysis, namely the long time behavior considering the least stable mode. However, the non self-adjoint nature of the linearized equations can lead to a significant transient energy growth before the eventual stable asymptotic behavior takes place. Concretely, small velocity perturbations in the direction normal to the shear redistribute the streamwise momentum, that lift-up effect leads to an algebraic growth of kinetic energy of three-dimensional disturbances. Such new formulation of the problem moves the issue on the initial condition. One solution is to look for the optimal perturbation,

namely the one that maximises the energy growth. This was introduced by Butler & Farrell [8] for plane shear flow and Schmidt & Henningson [9] for pipe flow. The optimal perturbations consist in streamwise elongated vortices which generate streamwise streaks. The streaks are then amplified, while the vortices are damped by viscosity. In absence of nonlinear feed-back to regenerate the vortices, the perturbations eventually evolves to asymptotic modal behaviour.

In order to determine the threshold of the initial perturbation energy above which the linear amplification is supplemented by nonlinear bootstrap, optimal perturbations have been extended to nonlinear equations for square duct flow [10]. However, parametric studies with direct numerical simulations on random initial perturbations have shown that the threshold is not unique for a given Reynolds number. In fact, the border separating the basin of attraction of the laminar state and the turbulence was found to be fractal [11]. Hence the definition of a critical Reynolds number depends on the receptivity process and needs a statistical approach.

Recently, Avila *et al.* [12] considered turbulence as statistically sustained when the lifetime of the spreading turbulence is greater than the lifetime of the decaying turbulence. In order to determine the onset of sustained turbulence, Avila *et al.* [12] obtained these two characteristic time scales, averaged over many experiments and simulations for various Reynolds numbers. As expected, the spreading probability increases with the Reynolds number while the probability to relaminarize decreases with it. Hence, the intersection of these two curves, at  $Re = 2040 \pm 10$ , marks the transition between transient and sustained turbulence in pipe flow. In contrast to the classical Landau-Ruelle-Takens view that turbulence arises from an increase in the temporal complexity of fluid motion, Avila *et al.* [12] show the transition as a spatial proliferation of chaotic domains.

The velocity field can be decomposed into a laminar part  $\mathbf{U}$  plus the turbulent fluctuations  $\mathbf{u}'$ . That separa-

ration is trivial for straight duct flows since the laminar solution remains stationary and the non streamwise components are nil for all Reynolds numbers. In the present article we consider a slightly square curved duct, which introduces a new parameter: the curvature ratio  $\epsilon = h/R \ll 1$  (see the scheme in figure 1). The curvature ratio is thus zero for a straight duct and tends to unity for a duct elbow. Usual non-dimensional set of

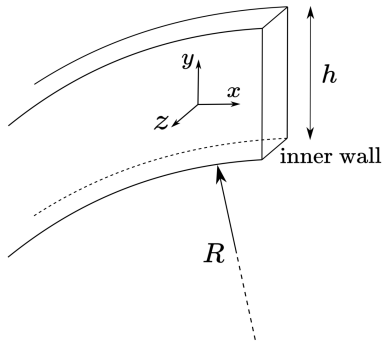


FIG. 1. Scheme and notations.

Cartesian coordinates  $(x, y, z)$  and velocity components  $\mathbf{u} = (u, v, w)$  are adopted in streamwise, wall-normal and spanwise directions respectively. In this work the definitions for the Reynolds and Dean numbers are the following:  $Re = U_b h / \nu$ ,  $De = Re \sqrt{h/R}$ , where  $U_b$  is the bulk velocity and  $\nu$  is the dynamic viscosity. The square duct configuration presents the advantage of having only a limited number of symmetries as compared to circular pipe flows. Despite these differences, the dynamics are in general analogous to those in circular pipes, for example the square duct flow is also linearly stable for any  $Re$  [10, 13]. For overviews on the subject, see Berger *et al.* [14], who present an extensive review on laminar flow in curved pipes, while Kalpakli Vester *et al.* [15] concentrate on the research concerning turbulent and transitional flows while providing a thorough historical review.

The aim of the present work is to understand the interaction between two separate phenomena that take place at the same time in turbulent flows in weakly bent pipes: the super-critical bifurcation to chaos of the laminar state (governed by the Dean number) and the sub-critical transition to turbulence (governed by the Reynolds number).

The weak curvature permits the decomposition of Navier-Stokes equation into a laminar set, sensitive to curvature effects and a turbulent set, not explicitly dependent on the curvature ratio. Indeed, the curvature influences the turbulent fluctuations only through the laminar part, which may be temporally complex. The model is obtained in the low curvature assumption, based on scales separation, neglecting the terms lower than  $\sqrt{h/R}$ .

The laminar component is solution of the following

equations [16]:

$$\begin{aligned} V_y + W_z &= 0 \\ U_t + VU_y + WU_z &= -\frac{dP_0}{dx} + Re^{-1} \Delta_2 U \\ V_t + VV_y + WV_z - \left(\frac{De}{Re} U\right)^2 &= -P_y + Re^{-1} \Delta_2 V \\ W_t + VW_y + WW_z &= -P_z + Re^{-1} \Delta_2 W \end{aligned} \quad (1)$$

with  $\Delta_2 = \partial^2 / \partial y^2 + \partial^2 / \partial z^2$ . The curvature is represented uniquely by the centrifugal term of the cylindrical Navier-Stokes equations,  $-(De/Re U)^2$ . Validations of this simplified model against available data in the literature are reported in [16]. The laminar solution is streamwise homogeneous, nonetheless the curvature may induce streamwise travelling-waves with very large streamwise scale and low amplitude. For the results shown in this article, the influence of these travelling-waves are negligible, thus we keep a two-dimensional laminar flow for simplicity.

The turbulent fluctuations satisfy the equations:

$$\begin{aligned} \nabla \cdot \mathbf{u}' &= 0 \\ \mathbf{u}'_t + (\mathbf{U} + \mathbf{u}') \cdot \nabla \mathbf{u}' + \mathbf{u}' \cdot \nabla \mathbf{U} &= -\frac{dp'_0}{dx} \mathbf{e}_x - \nabla p' + \frac{\nabla^2 \mathbf{u}'}{Re} \end{aligned} \quad (2)$$

This decomposition should be distinguished from the classical Reynolds Averaged Navier-Stokes equations. In RANS equations, mean flow is forced by the turbulent fluctuations, which is not the case for the laminar equations (1). As a result, the present model allows to investigate separately the curvature and turbulent effects.

Equations (1) and (2) are completed with no-slip boundary conditions on the four walls and a periodic boundary condition in the streamwise direction. Two different streamwise pressure gradients are present. The laminar pressure gradient  $-dP_0/dx$  is adjusted in such way that the non-dimensional laminar bulk velocity is unitary ( $U_b = \int_{yz} U dy dz = 1$ ). The pressure gradient of the fluctuations  $-dp'_0/dx$  is adjusted to ensure that  $u'_b = 0$ . The equations are solved with a spectral method in space and a backward Euler scheme in time [16].

The equations (1) for the laminar component involve two control parameters: the Reynolds number  $Re$  and the Dean number  $De$ . Nonetheless, it is possible to express the same equations only in terms of the Dean number by using boundary-layer type scaling (see [16]). Here, we keep the same scaling for the two systems (1) and (2) for convenience.

Thus, the laminar flow is fully characterised by the Dean number in the low curvature limit. Winters [17] presented for the first time a bifurcation diagram of the problem. Wang and Yang [18] provided a very detailed bifurcation diagram and identified regions of periodic and

chaotic oscillations. The first bifurcation from a steady regime to an unsteady, periodic regime occurs at  $De = 128$  through a saddle-node bifurcation. Starting from  $De = 193$  we observe two periods which are incommensurable, characteristic of an aperiodic regime. Then the system quickly evolves into chaos from  $De \approx 195$  [19].

In the following we consider two Dean numbers: 160 and 220, associated respectively to periodic and chaotic laminar states. In figure 2, we show the temporal evolution of the velocity difference  $\|\delta\mathbf{u}\|$  between two trajectories initially infinitesimally close. For the periodic regime ( $De=160$ ), the difference remains small while for chaotic regime an exponential increase is observed, illustrating the sensitive dependence upon initial conditions for the laminar solution at  $De=220$ .

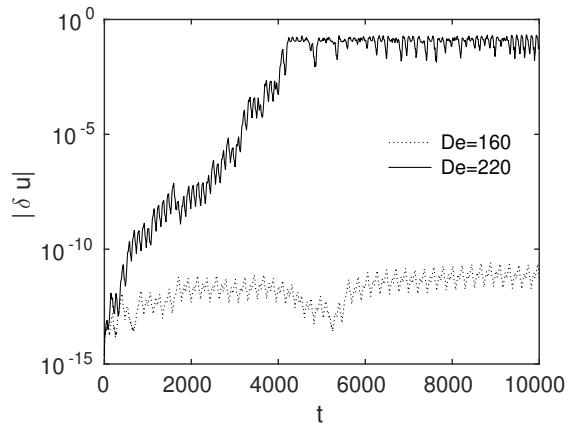


FIG. 2. The separation between two neighbouring trajectories plotted against time for two Dean numbers. At  $De=220$ , the sensitivity to initial condition illustrates the chaotic nature of the laminar solution.

The Reynolds number is fixed at 2500, large enough to observe developed turbulence. Although the bifurcation for laminar state state is supercritical, the turbulent state remains sub-critical, as observed for straight ducts, indeed, simulations with a linearized version of the equations 2 result in vanishing fluctuations.

As a first result, we consider the curvature effect of the duct on internal flow patterns at  $De=160$ . The organised fluid motions can be regarded as comprising two components, a primary streamwise flow and a secondary flow. These secondary flows are distinguished into first and second kind after Prandtl. The first kind secondary flow is a consequence of curvature. The centripetal acceleration  $-(De/Re U)^2$  is in equilibrium with the vertical pressure gradient  $-\partial P/\partial y$ . Because of the side walls, the pressure is non-homogeneous in the lateral direction  $-\partial P/\partial z \neq 0$  which induces a cross-flow. That mechanism is responsible of the so-called Dean two cells vortices [20–22]. Moreover, when the radial pressure gradient is strong enough, it can give rise to additional Taylor-Görtler vortices on the concave outer wall illustrated in figure 3, that shows

the time averaged laminar component of the flow. The presence of additional vortices results in complex laminar states which experience successive bifurcations between steady, unsteady and temporally chaotic regimes governed by the Dean number.

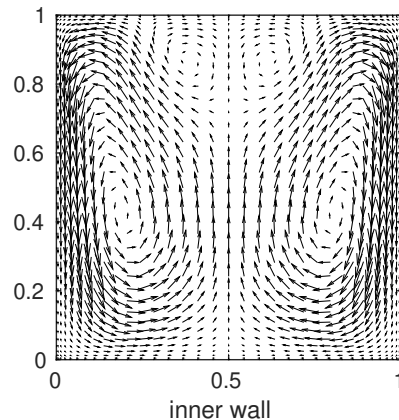


FIG. 3. Time averaged cross flow vortices. Laminar solution,  $Re=2500$ ,  $De=160$ .

The vortices of the second kind are a consequence of turbulence, as discovered by Prandtl in 1927. In turbulent regimes the average velocity field contains nonzero transverse components induced by the Reynolds shear stress [23]. Secondary motions in square ducts are known to come in the form of eight counter-rotating eddies bringing high-momentum fluid from the duct core towards the corners [24, 25]. Vortices of the second kind also occur in the presence of curvature; figure 4 shows the time averaged turbulent component of the flow. This

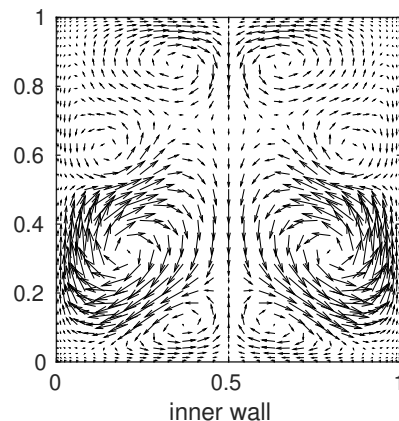


FIG. 4. Time averaged cross flow vortices. Turbulent part,  $Re=2500$ ,  $De=160$ .

observation is made possible by the introduction of the decomposition between the unsteady laminar and turbulent components. If such decomposition is not applied the laminar and turbulent effects can be hardly discrimi-

nated, which prevents the observation of the second kind motions. In a bent pipe their shape is topologically similar to the one of a straight duct, with the presence of eight streamwise vortices, that differ in position and size. The two pairs closer to the outer wall present vortices similar in size, whose separator is not aligned with the duct bisector as in the straight case, but has a different angle. This feature is even more evident for the two pairs closer to the inner wall, in which the upper vortex is much stronger than the lower one.

The laminar-turbulent decomposition also permits to analyse the pressure drop driving the flow. Both curvature and turbulent fluctuations increase the drag, and therefore also the pressure drop required to ensure a unitary bulk velocity. In figures 5 and 6, the temporal spectra of the laminar component  $-dP_0/dx$  and the turbulent component  $-dp'_0/dx$  are depicted for  $De=160$  and  $220$  respectively.

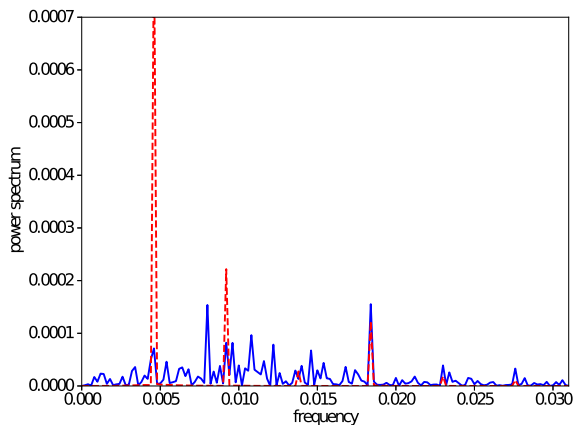


FIG. 5. Spectrum, laminar periodic (red discontinuous line) vs turbulent (blue continuous line), at  $Re=2500$ ,  $De=160$ .

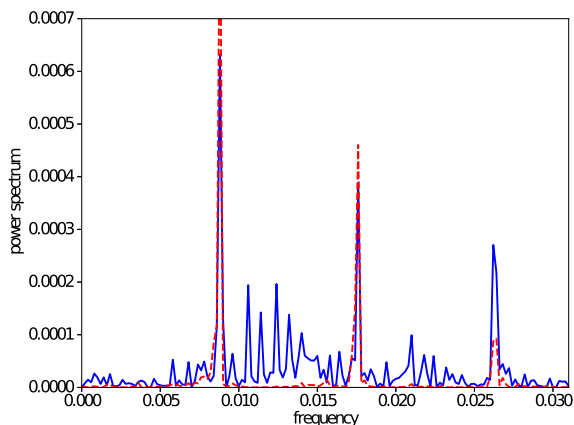


FIG. 6. Spectrum, laminar chaotic (red discontinuous line) vs turbulent (blue continuous line), at  $Re=2500$ ,  $De=220$ .

At  $De=160$ , the laminar pressure drop spectrum

presents the characteristics of a periodic signal, with sharp peaks at the fundamental frequency and the harmonics, while the turbulent signal shows a rather broadband spectrum. Figure 6 illustrates a different behaviour, the laminar part is characterised by two non commensurable frequencies (and their harmonics) while the turbulent part shows frequency synchronisation with the dominant laminar frequencies.

In conclusion, the laminar-turbulent decomposition allows to distinguish between the effects of curvature and turbulent fluctuations. Moreover, the model also reveals an alternative scenario for the transition to turbulence. In contrast to the classical Landau-Ruelle-Takens view that turbulence arises from an increase in the temporal complexity of fluid motion, starting with steady laminar flow, as described in [26, 27]; here we show that in a configuration with two control parameters the transition to chaos can be independently observed for both laminar and turbulent components.

\* damien.biau@ensam.eu

- [1] S. P. Suter and R. Skalak, The history of poiseuille's law, *Annu. Rev. Fluid Mech.* **25**, 1 (1993).
- [2] G. G. Stokes, On the theories of the internal friction of fluids in motion, and of the equilibrium and motion of elastic solids, in *Mathematical and Physical Papers*, Vol. 1 (Cambridge University Press, 2009) p. 75–129.
- [3] O. Reynolds, Xxix. an experimental investigation of the circumstances which determine whether the motion of water shall be direct or sinuous, and of the law of resistance in parallel channels, *Philos. Trans. Royal Soc.* **174**, 935 (1883).
- [4] N. Rott, Note on the history of the reynolds number, *Annual review of fluid mechanics* **22**, 1 (1990).
- [5] G. I. Taylor, Viii. stability of a viscous liquid contained between two rotating cylinders, *Philos. Trans. Royal Soc. A* **223**, 289 (1923).
- [6] H. Salwen, F. W. Cotton, and C. E. Grosch, Linear stability of poiseuille flow in a circular pipe, *J. Fluid Mech.* **98**, 273–284 (1980).
- [7] A. Meseguer and L. Trefethen, Linearized pipe flow to reynolds number  $10^7$ , *J. Comput. Phys.* **186**, 178 (2003).
- [8] K. M. Butler and B. F. Farrell, Three-dimensional optimal perturbations in viscous shear flow, *Phys. Fluids* **4**, 1637 (1992).
- [9] P. J. Schmid and D. S. Henningson, Optimal energy density growth in hagen–poiseuille flow, *J. Fluid Mech.* **277**, 197–225 (1994).
- [10] D. Biau and A. Bottaro, An optimal path to transition in a duct, *Philos. Trans. Royal Soc. A* **367**, 529 (2009).
- [11] A. Schmieguel and B. Eckhardt, Fractal stability border in plane couette flow, *Phys. Rev. Lett.* **79**, 5250 (1997).
- [12] K. Avila, D. Moxey, A. de Lozar, M. Avila, D. Barkley, and B. Hof, The onset of turbulence in pipe flow, *Science* **333**, 192 (2011).
- [13] T. Tatsumi and T. Yoshimura, Stability of the laminar flow in a rectangular duct, *J. Fluid Mech.* **212**, 437–449 (1990).

- [14] S. Berger, L. Talbot, and L. Yao, Flow in curved pipes, *Annual review of fluid mechanics* **15**, 461 (1983).
- [15] A. Kalpakli Vester, R. Örlü, and P. H. Alfredsson, Turbulent flows in curved pipes: recent advances in experiments and simulations, *Applied Mechanics Reviews* **68** (2016).
- [16] L. Rigo, D. Biau, and X. Gloerfelt, Flow in a weakly curved square duct: Assessment and extension of Dean’s model, *Physical Review Fluids* **6**, 024101 (2021).
- [17] K. H. Winters, A bifurcation study of laminar flow in a curved tube of rectangular cross-section, *J. Fluid Mech.* **180**, 343 (1987).
- [18] L. Wang and T. Yang, Bifurcation and stability of forced convection in curved ducts of square cross-section, *Int. J. Heat Mass Transf.* **47**, 2971 (2004).
- [19] It should be noted that Wang and Yang [18] use a different definition of the Dean number, the values reported have been converted to the definition used in this paper for simplicity.
- [20] W. Dean, Xvi. note on the motion of fluid in a curved pipe, *London Edinburgh Philos. Mag. J. Sci.* **4**, 208 (1927).
- [21] W. Dean, Lxxii. the stream-line motion of fluid in a curved pipe (second paper), *London Edinburgh Philos. Mag. J. Sci.* **5**, 673 (1928), <https://doi.org/10.1080/14786440408564513>.
- [22] W. R. Dean and J. M. Hurst, Note on the motion of fluid in a curved pipe, *Mathematika* **6**, 77–85 (1959).
- [23] P. Bradshaw, Turbulent secondary flows, *Annu. Rev. Fluid Mech.* **19**, 53 (1987).
- [24] S. Gavrilakis, Numerical simulation of low-reynolds-number turbulent flow through a straight square duct, *J. Fluid Mech.* **244**, 101–129 (1992).
- [25] A. Huser and S. Biringen, Direct numerical simulation of turbulent flow in a square duct, *J. Fluid Mech.* **257**, 65 (1993).
- [26] J. Kühnen, P. Braunschier, M. Schwegel, H. C. Kuhlmann, and B. Hof, Subcritical versus supercritical transition to turbulence in curved pipes, *J. Fluid Mech.* **770**, R3 (2015).
- [27] J. Canton, E. Rinaldi, R. Örlü, and P. Schlatter, Critical point for bifurcation cascades and featureless turbulence, *Phys. Rev. Lett.* **124**, 014501 (2020).